Catalytic activity of supported solid catalysts for phenol hydroxylation

**B. P. Nethravathi · K. Ramakrishna Reddy ·
K. N. Mahendra**

Abstract Cobalt(II), copper(II) and zinc(II) complexes of 2-phenylbenzimidazole (PhBzlH) encapsulated in the supercages of zeolite-Y and ZSM-5 have been synthesized and characterized by spectroscopic studies (IR, UV/visible, EPR), elemental analyses, thermal studies and X-ray diffraction patterns. The catalytic activity of encapsulated complexes was investigated for the hydroxylation of phenol using 30 % H_2O_2 as an oxidant. Under optimized reaction conditions, the hydroxylation of phenol yielded catechol and hydroquinone as the major products. All catalysts show good selectivity for diphenol products. A maximum conversion of phenol was obtained with [Cu(PhBzlH)]-Y as the catalyst. The results showed that conversion of phenol varies in the order [Cu(PhBzlH)]-Y (53 %) > [Cu(PhBzlH)]-ZSM-5 > (49 %) > [Co(PhBzlH)]-ZSM-5 (47 %) > [Co(PhBzlH)]-Y (46 %) > [Zn(PhBzlH)]-Y (45 %) > [Zn(PhBzlH)]-ZSM-5 (41 %) after 6 h of reaction time. Test for the recyclability of the reaction was also carried out and the results indicate their recyclability.

Keywords Zeolite · Encapsulation · Hydrogen peroxide · Catalyst · Phenol

B. P. Nethravathi
Department of Chemistry, Vijaya College, R.V. Road,
Bangalore 560 004, India

K. Ramakrishna Reddy
Department of Chemistry, Government Science College,
Bangalore 560 001, India

K. N. Mahendra (✉)
Department of Chemistry, Bangalore University,
Bangalore 560 001, India
e-mail: knmahendra@gmail.com

1 Introduction

Immobilization of homogeneous catalysts to a solid support has received wide attention as these materials have advantages of both homogeneous and heterogeneous catalysis. The supported catalysts enhance their thermal stability, selectivity, recyclability and easy separation from reaction products. The non corrosive, environment friendly and economically viable nature of the zeolite catalysed reactions also lead them to use in various industrial processes such as catalytic cracking, hydrocracking, isomerization and oxidation [1]. Zeolite encapsulated metal complexes are one of such materials for heterogeneization of homogeneous catalysts. These zeolite encapsulated metal complexes were used in various organic reactions like carbonylation, hydroformylation, hydrogenation, oxidation, hydroxylation etc. [2–8].

Use of solid catalysts for selective oxidation of phenols preferably at near—ambient conditions and using clean oxidants like O_2 or H_2O_2 is a research area of growing importance. Hydroxylation of phenol with H_2O_2 using microporous titanosilicate, TS-1 and its commercial utilization by Erichem workers [9] is a major advance in this area. Hydroquinone and catechol are obtained with high selectivity over TS-1. Strong mineral acids or Fenton's reagent are other efficient catalysts for the hydroxylation of phenol using H_2O_2 as the oxidant, producing peroxonium ion and hydroxyl radical, respectively. Various metal phthalocyanines have been studied for the hydroxylation of phenol by H_2O_2 [10]. It was found that the metal ion of the catalyst influences both activity and selectivity of the reaction as well as the distribution of catechol and hydroquinone. Since H_2O_2 alone is not a hydroxylating agent, catalysts have to be added to make it a hydroxylating agent. An active oxidant for the hydroxylation of phenol is an

🖄 Springer
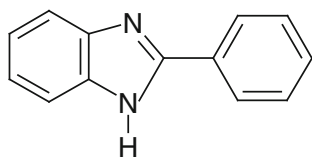
Scheme 1 2-phenylbenzimidazole (PhBzlH)

ionic species formed by the activation or reaction of H_2O_2 with metal phthalocyanines. Bimetallic Sn–Mo and Sn–Sb phthalocyanines have also been used to hydroxylate phenols using H_2O_2 as the oxidant [11].

Already we reported the heterogeneous catalytic system by preparing Co(II), Cu(II) and Zn(II) complexes of 2-methyl and 2,2-aminophenylbenzimidazole in the supercages of zeolite Y and ZSM-5 and catalytic activity for the oxidation of phenol studied [12, 13]. Synthesis and characterization of 2-phenylbenzimidazole complexes were reported earlier [14], but they have not reported as zeolite encapsulated complexes.

In this work, studies on the synthesis and characterization of zeolite Y and ZSM-5 encapsulated complexes of Co(II), Cu(II) and Zn(II) with 2-phenylbenzimidazole ligand (PhBzlH) are presented. The structure of the 2-phenylbenzimidazole ligand (PhBzlH) was shown in Scheme 1. Applications of these complexes for hydroxylation of phenol was studied and the results of these studies are discussed.

2 Experimental section

2.1 Materials

Protonated form of zeolite Y [H-Y] [Si to Al ratio 5.07] and ZSM-5 [H-ZSM-5] [Si to Al ratio 21.31] were purchased from Sud-Chemie, Mumbai. L R–Grade solvents used were purified according to the literature method [15]. The chemicals used for the studies were of AR grade and purchased from Merck. 2-phenylbenzimidazole was prepared according to the literature method [16].

2.2 Physicochemical characterization

The metal content was estimated using Perkin–Elmer model ICP-AES instrument. The surface areas of the zeolite samples were determined by the BET method of nitrogen adsorption at liquid nitrogen temperature by BET method on a NOVA-1000 Ver. 3.70 instrument. Powder X-ray diffraction patterns of zeolite HY, H-ZSM-5 and the zeolite encapsulated complexes were recorded using Philips X'Pert diffractometer using CuK_{α} ($\lambda = 0.15405$ nm) target with nickel filter. Thermogravimetric analysis was

recorded on a NETZSCH STA 409 PG/PC under nitrogen atmosphere for the encapsulated complex with the heating rate of 10 °C/min from 30 to 800 °C. The morphology of the sample was examined using Philips scanning electron microscopy. Infrared spectra of the ligand, simple complex and supported complexes in the region 4,000–400 cm^{-1} were recorded as KBr pellet on a FTIR-8400S Shimadzu, spectrophotometer. The diffuse reflectance spectra were recorded at room temperature in the range 200–800 nm using $BaSO_4$ as reference on a Shimadzu UV–Visible-NIR model UV-3101P instrument. The X-band EPR spectra of powdered samples of zeolite encapsulated Cu(II) complexes were recorded at room temperature on a VARIAN E-112 ESR spectrometer and the g values were estimated relative to tetracyanoethylene (TCNE, g = 2.0027). Shimadzu 14B gas chromatograph fitted with FID detector connected with BP-5 capillary column was used to analyze the reaction products of the catalytic activity studies.

2.3 Preparation of complexes

Protonated form of zeolite Y (H-Y) or H-ZSM-5 (5 g) sample was stirred in an aqueous solution of the respective metal salt taken in a 100 ml round bottom flask. The mixture was refluxed with stirring for 12 h on an oil bath. It was filtered and washed with water till the washings were free from metal ions and then dried in an oven at 150 °C for 24 h. This metal exchanged zeolite was treated with 2-phenylbenzimidazole in acetone medium and then refluxed with stirring for 24 h on an oil bath. The reaction mixture was filtered, washed with DMF and then with acetone using Soxhlet apparatus to remove any unreacted ligand and the metal complex adsorbed on the zeolite surface. The resulting solution was treated with aqueous 0.01 M NaCl with stirring for 15 h to allow exchange of uncomplexed metal ions with sodium ions. The zeolite encapsulated complex was then filtered, washed with distilled water to remove any chloride ions present and dried at 150 °C for 24 h.

2.4 Catalytic activity measurements

2.4.1 Decomposition of H_2O_2

An aqueous solution of 30 % H_2O_2 (4 ml, 5.54 g) was added to 2 mmol catalyst and it was stirred for 1 and 2 h at room temperature. The catalyst was then separated out by filtration and washed with distilled water. The filtrate containing partially decomposed H_2O_2 and the washings were collected in a 250 ml volumetric flask, and then made up to the mark with distilled water. Then 10 ml of this solution was titrated against standard $KMnO_4$ solution to estimate the unreacted H_2O_2 [17].

Table 1 Percentage of metal, colour and the surface area measurement data

Sl. no.	Compound	Colour	Metal (wt%)	S_{BET} $(m^2/g)^a$	Pore volume $(cc/g)^b$
1	H-Z-Y[c]	White	–	25.8	0.105
2	H-ZSM-5[d]	White	–	258.7	0.179
3	[Co(PhBzlH)]-Y	Pink	0.935	20.41	0.095
4	[Co(PhBzlH)]-ZSM	White	0.037	122.3	0.100
5	[Cu(PhBzlH)]-Y	Dirty white	3.135	15.13	0.035
6	[Cu(PhBzlH)]-ZSM-5	Dirty white	0.089	78.23	0.098
7	[Zn(PhBzlH)]-Y	White	2.314	23.80	0.052
8	[Zn(PhBzlH)]-ZSM-5	White	0.245	192.98	0.152

[a] S_{BET} = specific surface area measured by BET method

[b] Pore volume calculated from N_2 desorption by the BJH method

[c] H-Z-Y and [d] H-ZSM-5 = protonated form of zeolite-Y and ZSM-5

2.4.2 Hydroxylation of phenol

The reactions were carried out in a 50 ml double-necked round bottom flask fitted with a water cooled condenser. In a typical reaction, phenol (2.35 g, 0.025 mol) and 30 % aqueous H_2O_2 (4 ml, 0.05 mol, 5.54 g) were dissolved in 2 ml of acetonitrile and the reaction mixture was heated on an oil bath at 80 °C with continuous stirring. Then 2.5 mmol of the catalyst was added and the reaction was considered to begin. Aliquots were drawn from the reaction mixture at regular intervals for analysis using a gas chromatograph.

3 Results and discussion

3.1 Synthesis and characterization of catalysts

Synthesis of the metal complexes encapsulated in the zeolite cages of H-Y and H-ZSM-5 was carried out by the flexible ligand method [18]. The metal content in the encapsulated complex was determined by using the ICP instrument. The analysis of metal content along with the colour of the complexes and the surface area measurements are given in Table 1.

To compare the properties of neat with encapsulated complexes, the neat complexes of Co(II), Cu(II) and Zn(II) with PhBzlH were also prepared and characterized by various physicochemical techniques. The analytical data proposed is in good agreement with the data available in literature [14].

The significant reduction in surface area and pore volume as a result of encapsulation of complexes within the
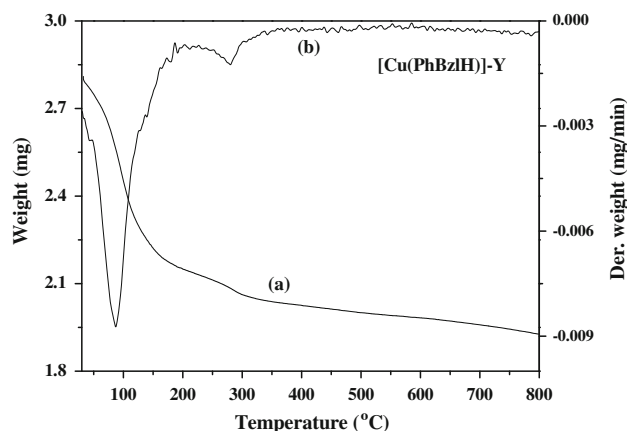
Fig. 1 *a* TGA and *b* DTG *curves* of [Cu(PhBzlH)]-Y

Table 2 Thermogravimetric analysis data of encapsulated PhBzlH complexes

Sl. no.	Complex	Temperature range (°C)	Weight loss (%)	Group lost
1	[Co(PhBzlH)]-Y	56–170	15.52	nH_2O
		170–340	5.48	$H_2O + Cl^-$
		340–690	1.61	L
2	[Co(PhBzlH)]-ZSM-5	52–185	3.8	nH_2O
		185–628	4.1	$H_2O + Cl^-$
		628–725	0.29	L
3	[Cu(PhBzlH)]-Y	32–184	22.86	nH_2O
		184–315	3.93	H_2O
		315–800	4.28	L
4	[Cu(PhBzlH)]-ZSM-5	38–206	7.39	nH_2O
		206–607	5.65	H_2O
		607–800	2.39	L
5	[Zn(PhBzlH)]-Y	43–216	18.58	nH_2O
		216–655	6.80	H_2O
		655–800	1.20	L
6	[Zn(PhBzlH)]-ZSM-5	36–148	6.0	nH_2O
		148–645	7.11	H_2O
		645–800	1.12	L

L Ligand

zeolite pores is due to the blocking of the pores by the formation of the metal complexes [19]. The decrease in surface area values suggests the formation of metal complexes inside the zeolite cages.

3.2 Thermogravimetric analysis

Thermal stability of the encapsulated complex was studied using TGA and DTG. Representative TGA and DTG curves

of the [Cu(PhBzlH)]-Y complex are shown in Fig. 1. The thermogravimetric analysis data for all the complexes are presented in Table 2. The weight loss of the encapsulated complexes can be clearly observed in DTG and it occurs in two or three steps in the temperature range of 32–800 °C. All the encapsulated complexes show almost similar decomposition pattern. The first stage of mass loss up to around 200 °C corresponds to the removal of lattice water molecule present in zeolite cavities [5]. In the second stage, expel of coordinated water molecules (if any) and anions can be expected. So, the encapsulated complexes decompose only at a higher temperature than that for the simple complexes. Due to the encapsulation, complexes become more thermally stable. A very small weight loss was observed and it may be due to the presence of low metal complex in the zeolite cavities [1]. This is in agreement with the low metal content as estimated by the ICP instrument.

3.3 Powder X-ray diffraction studies

The powder X-ray diffraction patterns of H-Y, H-ZSM-5 and the encapsulated complexes were recorded at 2θ values of 5–80°. Essentially very similar patterns are formed for the encapsulated complexes as compared to the starting zeolite H-Y and H-ZSM-5, though slight changes in the intensity of the bands are seen. These observations indicate that the crystalline nature of the zeolite is retained even after the encapsulation of the complex. No new peaks were detected in the XRD patterns of the encapsulated complex possibly due to the presence of low content of the metal complexes.

3.4 Infrared spectral studies

The selected spectral data is presented in the Table 3. The infrared spectral data of the ligand and complexes reveal the co-ordination of the ligand to the metal ion. The infrared spectra of the ligand exhibit a band at around 3,050 cm^{-1}, assigned to $\nu_{(NH)}$. The lowering of this band frequency is due to association through the intermolecular hydrogen bonding [20]. The $\nu_{(C=N)}$ and $\nu_{(C=C)}$ vibrations are very close and occur around 1,620 cm^{-1}. The band around 1,590 cm^{-1} is assigned to the NH in-plane bending. Another band appearing at 1,541 cm^{-1} may be due to δ_{C-H} vibration. The ν_{C-N} and δ_{N-H} appear around 1,313 cm^{-1}. The Substituted phenyl group shows ring vibrations at 1,485 and 740 cm^{-1}. The bands around 1,409, 1,276, 1,002, 615 and 430 cm^{-1} are assigned to the benzimidazole ring vibrations. The weak band around 780 cm^{-1} is ascribed to NH out-of-plane bending vibration.

The infrared spectra of the complexes are similar to those of the corresponding ligands. An upward shift (5–15 cm^{-1}) of the $\nu_{(C=N)}$ in the IR spectra of the complexes as compared to their values in the free ligand, suggests coordination through the pyridine nitrogen of imidazoline. The other bands in the spectrum of each complex are similar to those in the corresponding ligand spectrum except for slight shifts in their positions and changes in their intensities due to coordination. These empirical band assignments have been made on the basis of earlier reported assignments by other workers earlier [14, 21].

All metal complexes encapsulated in zeolites exhibit bands around 1,100, 950, 800 and 750 cm^{-1} which arise from zeolite framework. We have not observed any broadening and shift in the positions of the zeolite vibrational bands, which indicates that no change has occurred in the zeolite framework. This clearly indicates that, the metal complexes fit well within the cavities of the zeolites.

3.5 Electronic spectral studies

The electronic spectral data of ligand, neat and encapsulated complexes recorded using BaSO$_4$ as references are given in Table 4.

Table 3 Partial IR spectral data of PhBzlH and its complexes

Compound	ν_{N-H} (cm^{-1})	$\nu_{C=N}/\nu_{C=C}$ (cm^{-1})	N–H in-plane bending (cm^{-1})	δ_{C-H} (cm^{-})	ν_{C-N}/δ_{N-H} (cm^{-1})	N–H out-of-plane-bending (cm^{-1})
PhBzlH	3,045	1,617	1,587	154	1,308	787
[Co(PhBzlH)]	3,055	1,629	1,573	1,540	1,309	781
[Co(PhBzlH)]-Y	a	1,629	1,577	1,540	1,307	a
[Co(PhBzlH)]-ZSM	a	1,635	1,560	1,541	a	a
[Cu(PhBzlH)]	3,056	1,629	1,566	1,544	1,309	777
[Cu(PhBzlH)] -Y	a	1,624	1,570	1,540	1,311	a
[Cu(PhBzlH)]-ZSM	a	1,628	1,570	1,544	1,330	a
[Zn(PhBzlH)]	3,055	1,620	1,587	1,542	1,310	781
[Zn(PhBzlH)]-Y	a	1,630	1,578	1,544	1,313	a
[Zn(PhBzlH)]-ZSM	a	1,637	1,579	1,550	1,311	a

a = bands not resolved due to overlap with zeolite bands

Table 4 Electronic spectral data of PhBzlH and its complexes

| Sl. no.	Compound	λ_{max} (nm)	Tentative assignments
1	[Co(PhBzlH)]	658	d–d
2	[Co(PhBzlH)]-Y	520	d–d
3	[Co(PhBzlH)]-ZSM	374	Charge transfer
		581	d–d
4	[Cu(PhBzlH)]	397	Charge transfer
		614	d–d
5	[Cu(PhBzlH)]-Y	413	Charge transfer
		765	d–d
6	[Cu(PhBzlH)]-ZSM	377	Charge transfer
		765	d–d
7	[Zn(PhBzlH)]	380	Charge transfer
8	[Zn(PhBzlH)]-Y	–	–
9	[Zn(PhBzlH)]-ZSM	395	Charge transfer

The electronic spectrum of the PhBzlH exhibits three peaks at 213, 250 and 300 nm due to $\pi - \pi^*$ transitions of benzimidazole moiety. Due to the low intensity of the observed bands some uncertainties arise in the detailed assignments of the bands for the complexes. The bands at higher frequencies can be due to charge transfer transitions, which is evident from the high intensity of these bands.

The electronic spectrum of cobalt (II) neat complex is characterized by the highest energy $^4A_2 \rightarrow {}^4T_{1(P)}$ transition at 658 nm is typical of tetrahedral Co(II) complexes [22]. Similar observations were made in the case of encapsulated complexes which suggest that the cobalt complex with tetrahedral geometry were formed inside the zeolite cavities. A broad band observed around 614 nm in neat Cu(II) complex is assigned to the $^2B_{1g} \rightarrow {}^2A_{1g}$ transition. In case of encapsulated complexes the bands are observed at 765 nm with an additional charge transfer transition band. The transition observed supports a square planar geometry for the copper complex formed inside the zeolite cavities [23].

The white coloured neat and encapsulated complexes of Zn(II) shows three bands at around 217–300 nm due to the π–π^* transitions of benzimidazole moiety. As expected no bands due to d–d transitions are observed in case of neat and encapsulated Zn(II) complexes [23] and the Zn(II) neat complex has a tetrahedral configuration which is realized by participation of the pyridine nitrogen of two organic ligand molecules, and two nitrate anions, typical for these classes of organic ligands [14].

3.6 EPR spectra

The EPR spectra of Cu(II) encapsulated complexes were recorded at room temperature using TCNE as reference. The spectra obtained are as shown in Figs. 2 and 3.
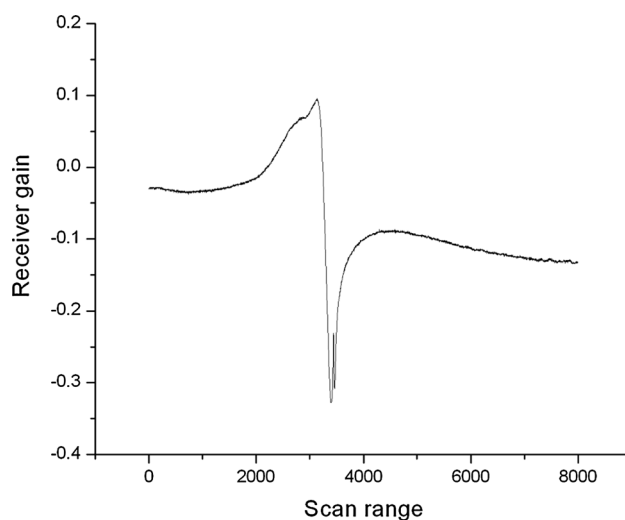
Fig. 2 EPR spectrum of [Cu(PhBzlH)] complexes
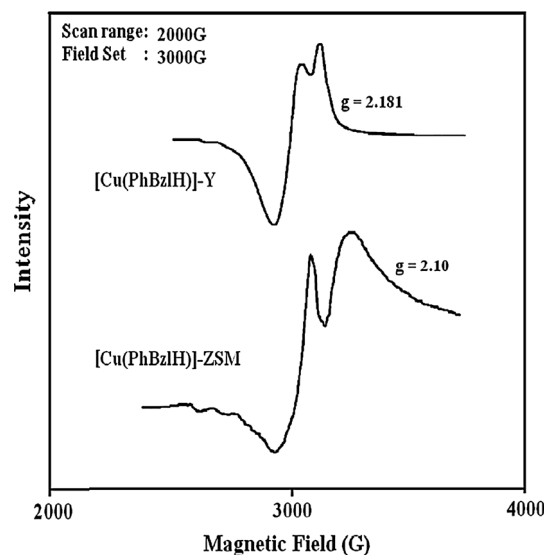
Fig. 3 EPR spectrum of Cu encapsulated PhBzlH complexes

Neat complexes showed broad EPR spectra corresponding to nearest neighbor spin–spin interactions and the g average is found to be 2.19. Whereas in the zeolite-encapsulated metal complexes the g average values are found to be 2.18 and 2.10 for ZY and ZSM-5 complexes. The spectra of encapsulated complexes are almost similar to that of the neat complexes. The g values of the zeolite-encapsulated complexes are similar to that of the neat complexes [24].

For copper complexes the g values are found to be 2.18 and 2.10 and are <2.3 indicating that these complexes possess considerable covalent character in the metal ligand bond. The interactions of the zeolite framework with the

encapsulated complex could induce some distortions in the expected structure.

3.7 Catalytic activity studies

3.7.1 Decomposition of H₂O₂

The catalytic activity for the decomposition of H_2O_2 with the encapsulated complexes was studied. The quantity of H_2O_2 that reacted and the turn over frequency (TOF) at two different time intervals (1 and 2 h) were measured. The results are tabulated in Table 5, which shows that the decomposition of H_2O_2 is slow initially but increases with time. This is due to the fact that the encapsulated complex used requires relatively longer time to exhibit maximum catalytic activity as the number of metal centers is less compared with that of the neat complex [25]. Hence increasing the duration of the reaction is a very effective way of carrying out the reaction with H_2O_2 as the source of oxygen.

3.7.2 Hydroxylation of phenol

The catalytic hydroxylation of phenol using different encapsulated complexes was studied as a function of time using H_2O_2 as the oxidant and acetonitrile as the solvent. Catechol and hydroquinone were obtained as the major products, as shown in Scheme 2. No minor products were detected in GC under the conditions employed here.

The reaction was carried out for 6 h of reaction time with the optimized condition (2.35 g phenol, 4 ml H_2O_2, 2.5 mmol catalyst in 2 ml of acetonitrile at 80 °C) for all the catalysts. The effect of different catalysts on the conversion of phenol and percentage selectivity of catechol and hydroquinone is represented in Fig. 4.

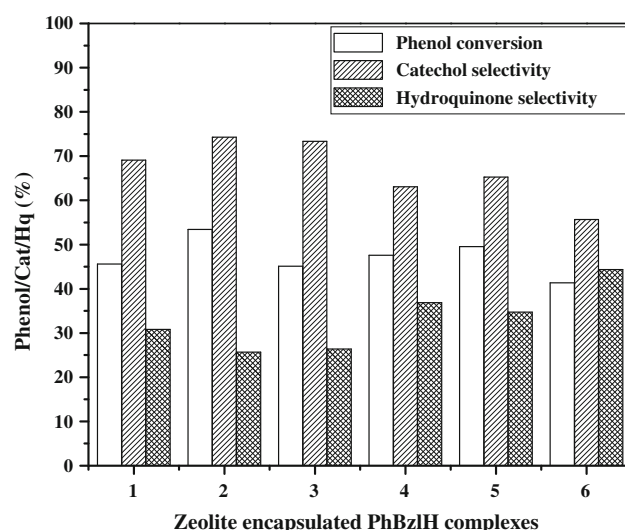The maximum conversion of phenol obtained is with [Cu(PhBzlH)]-Y. The order of catalytic activity for hydroxylation of phenol is found to be as follow. [Cu(PhBzlH)]-Y (53 %) > [Cu(PhBzlH)]-ZSM-5 > (49 %) > [Co(PhBzlH)]-ZSM-5 (47 %) > [Co(PhBzlH)]-Y (46 %) >[Zn(PhBzlH)]-Y (45 %) > [Zn(PhBzlH)]-ZSM-5 (41 %) after 6 h of reaction time. The different performance of the individual catalysts may be attributed to the d configuration of the metal ion/atom in the complex and geometry of the respective metal complexes [26].

A maximum conversion of 40 % to catechol and 14 % to hydroquinone formation was obtained with [Cu(PhBzlH)]-Y as catalyst. The order of catechol formation with different catalysts is as follows: [Cu(PhBzlH)]-Y > [Zn(PhBzlH)]-Y > [Cu(PhBzlH)]-ZSM > [Co(PhBzlH)]-Y > [Co(PhBzlH)]-ZSM > [Zn(PhBzlH)]-ZSM.

The hydroquinone formation for different catalysts employed follows the order as below: [Zn(PhBzlH)]-ZSM > [Co(PhBzlH)]-ZSM > [Cu(PhBzlH)]-ZSM > [Co(PhBzlH)]-Y > [Cu(PhBzlH)]-Y > [Zn(PhBzlH)]-Y. In all the catalysts, the selectivity is much more for catechol than hydroquinone.
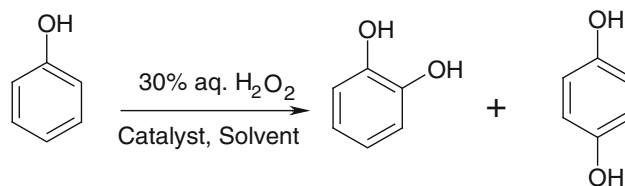
Scheme 2 Hydroxylation of phenol

Table 5 Percentage decomposition of H_2O_2

Catalyst[a]	After 1 h		After 2 h	
	H_2O_2 reacted (%)	TOF (h^{-1})[b]	H_2O_2 reacted (%)	TOF (h^{-1})[b]
[Co(PhBzlH))]-Y	0.160	66.72	1.45	300.38
[Co(PhBzlH))]-ZSM	14.160	36.00	18.03	22.91
[Cu(PhBzlH))]-Y	1.836	241.39	4.173	274.31
[Cu(PhBzlH))]-ZSM	14.39	47.53	77.78	44.66
[Zn(PhBzlH))]-Y	2.34	429.41	2.587	475.42
[Zn(PhBzlH))]-ZSM	14.416	6.225	17.025	3.676

TOF = moles of the substrate converted per mole of the (metal) in the solid catalyst per hour

Fig. 4 Comparison of phenol conversion and catechol and hydroquinone selectivity with zeolite encapsulated complexes of PhBzlH

3.8 Recycling test

Used catalysts were tested for their recyclability. The catalyst was separated after the reaction and was washed with acetonitrile, dried and used again with fresh reaction mixture, under the same optimized reaction condition. The products obtained were analyzed using GC. It was found that the phenol conversion was almost the same as that of the fresh run. The above procedure was repeated three times and we did not observe any loss in the catalytic activity of the encapsulated catalyst.

Leaching or decomposition of the catalysts was tested by considering blank reaction i.e. using 30 % aqueous H_2O_2 (0.25 mol), catalyst (2 mmol) in 2 mL of acetonitrile at 80 °C for 6 h. Absence of metal ions in mother liquor suggests no leaching or decomposition of complexes during catalytic activity.

4 Conclusions

Physical and spectral studies of the encapsulated zeolite clearly indicate that the encapsulation of complex occurs in the cages of zeolite. The encapsulated complexes are active catalysts for the decomposition of H_2O_2 and for the oxidation of phenol with good selectivity to catechol than hydroquinone. The IR and UV spectra of fresh and used catalysts are nearly identical with not much loss in intensity of the peaks, which indicate that these zeolite encapsulated transition metal complexes can be reused for catalytic study.

References

1. M.R. Maurya, S.J.J. Titinchi, S. Chand, Appl. Catal. A: Gen. **228**, 177 (2002)
2. P. Gellin, C. Naccache, Y.B. Taarit, Pure Appl. Chem. **8**, 1315 (1988)
3. M. Iwamoto, H. Kusano, S. Kagawa, Inorg. Chem. **22**, 3366 (1983)
4. S.R. Kowalak, C. Weiss, K.J. Balkus Jr, J. Chem. Soc. Chem. Commun. 57 (1991)
5. C. Ratnasamy, A. Murugkar, S. Padhye, Ind. J. Chem. **35A**, 1 (1996)
6. T. Joseph, C.S. Sajanikumari, S.S. Desh Pande, S. Gopinathan, Ind. J. Chem. **38A**, 792 (1999)
7. N. Ulgappan, V. Krishnasamy, Ind. J. Chem. **35A**, 787 (1996)
8. C. Bronnimann, T. Mallat, A. Baiker, J. Chem. Soc. Chem. Commun. **1377** (1995)
9. Y. Masri, M. Hronee, Stud. Surf. Sci. Catal. **66**, 455 (1991)
10. S. Alexander, B. Meunier, J. Chem. Soc., Chem. Commun. **15**, 1799 (1994)
11. M. Hronee, G. Kiss, J. Sitek, J. Chem. Soc., Faraday Trans. **1**(79), 1091 (1983)
12. B.P. Nethravathi, K.N. Mahendra, J. Porous Mater. **17**, 107 (2010)
13. B.P. Nethravathi, K. Ramakrishna Reddy, K.N. Mahendra, J. Porous Mater. **18**, 389 (2011)
14. S.O. Podunavac-Kuzmanovic, L.S. Vojinovic, APTEFF **34**, 119 (2003)
15. D.D. Perrin, W.L.F. Armanego, D.R. Perrin, *Purification of Laboratory Chemicals* (Pergamon Press, Oxford, 1966)
16. D.W. Hein, R.J. Alheim, J.J. Leavitt, J. Am. Chem. Soc. **79**, 427 (1957)
17. J. Bassett, R.C. Denney, G.H. Jeffery, J. Mendham, *Vogel's Textbook of Quantitative Inorganic Analysis*, 4th edn. (Longman Scientific and Technical, London, 1978)
18. C. Subrahmanyam, B. Louis, B.Viswanathan, A. Renken, T.K. Varadarajan, Bull. Catal. Soc. India 3 (2004)
19. K.J. Balkus Jr, A.G. Gabrielov, J. Inclusion Phenom. Mol. Recogn. Chem. **21**, 159 (1995)
20. X.K. Nakamoto, *Infrared and Raman Spectra of Inorganic and Coordination Compounds* (Wiley, New Yark, 1986)
21. S. Rekha, K.R. Nagasundara, Ind. J. Chem. **45A**, 2421 (2006)
22. S. Konstantinovic, C. Radovanovic, Z. Capic, V. Basic, J. Serb. Chem. Soc. **68**, 641 (2003)
23. K. Rama Krishna Reddy, K.N. Mahendra, Russ. J. Inorg. Chem. **53**(6), 906 (2008)
24. S. Deshpande, D. Srinivas, P. Ratnasamy, J. Catal. **188**, 261 (1999)
25. M.R. Maurya, S.J.J. Titinchi, S. Chand, J. Mol. Catal. Chem. **193**, 165 (2003)
26. K.N. Vinod, P. Puttaswamy, K.N.N. Gowda, Ind. Eng. Chem. Res. **49**, 3137 (2010)